C. R. Chimie 13 (2010) 731–736

Contents lists available at ScienceDirect

Comptes Rendus Chimie

www.sciencedirect.com

Preliminary communication/Communication

Lanthanide-doped $LiYF_4$ nanoparticles: Synthesis and multicolor upconversion tuning

Juan Wang [a], Feng Wang [a], Jun Xu [b], Yong Wang [b], Yongsheng Liu [c], Xueyuan Chen [c], Hongyu Chen [b], Xiaogang Liu [a,*]

[a] Department of Chemistry, National University of Singapore, Singapore 117543
[b] Division of Chemistry and Biological Chemistry, Nanyang Technological University, Singapore 637371
[c] Key Laboratory of Optoelectronic Materials Chemistry and Physics, Fujian Institute of Research on the Structure of Matter, Chinese Academy of Sciences, Fuzhou, Fujian 350002, China

ARTICLE INFO

Article history:
Received 12 December 2009
Accepted after revision 19 March 2010
Available online 7 May 2010

Keywords:
Tetragonal phase
$LiYF_4$
Monodisperse
Upconverting
Upconversion
Lanthanide doping

ABSTRACT

We report the synthesis of tetragonal-phase $LiYF_4$ nanoparticles doped with upconverting lanthanide ions. The nanoparticles have been characterized by XRD, TEM, and luminescence decay studies. The size of the as-synthesized $LiYF_4$ nanoparticles can be tuned by varying the precursor ratio of F to lanthanide ions. Passivated by oleic acid ligands, the $LiYF_4$ nanoparticles can be readily dispersed in a wide range of nonpolar solvents including hexane, cyclohexane, dichloromethane, and toluene. The lanthanide-doped (Yb^{3+}, Er^{3+}, Tm^{3+}, Ho^{3+}) $LiYF_4$ nanoparticles show intense upconversion emissions upon near infrared excitation at 980 nm. By varying composition and concentration of the dopant ions, the color output can be precisely modulated under single wavelength excitation with a diode laser.

1. Introduction

Over the past decade, lanthanide-doped nanoparticles have left their mark as efficient luminescent nanomaterials [1]. In contrast to conventional luminescent materials, such as fluorescent organic dyes and semiconducting nanoparticles, lanthanide-doped nanoparticles generally offer narrow emission bands, long luminescence lifetimes (micro- to millisecond range), low toxicity, as well as high resistance to photobleaching, blinking, and photochemical degradation [2]. In particular, the lanthanide-doped nanoparticles comprising proper host–dopant combinations can convert near infrared long-wavelength excitation radiation into shorter-wavelength visible emissions [3]. These unique anti-Stokes emitters, now widely known as upconversion nanoparticles, have evolved as a rapidly growing field and opened up the opportunity for creating new applications in diverse fields such as displays, solar cells, and biological assays [4].

Upconversion nanoparticles are typically composed of an inorganic host lattice and lanthanide dopant ions embedded in the host lattice [3]. Although the upconversion process primarily makes use of the ladder-like arranged 4f energy levels of the lanthanide dopant ions, the host lattice can significantly alter the upconversion processes by exerting a crystal field around the dopant ion and subtracting excitation energy of the dopant ion through lattice vibration. Therefore, a selection of appropriate host materials is essential in the synthesis of lanthanide-doped nanoparticles with favorable optical properties such as high upconversion efficiency and controllable emission profile. Upconversion emissions have been observed for a wide variety of host materials including oxides, bromides, chlorides, and fluorides [5]. Fluorides are commonly studied due to their low phonon energy and relatively high chemical stability [6]. For example, $NaYF_4$ has been generally regarded as the most efficient upconversion host for practical applications. To

* Corresponding author.
E-mail address: chmlx@nus.edu.sg (X. Liu).

1631-0748/$ – see front matter
doi:10.1016/j.crci.2010.03.021

this regard, considerable efforts have been devoted to the synthesis and multicolor tuning of lanthanide-doped $NaYF_4$ upconversion nanoparticles [7].

As one of the most efficient host materials for upconversion process, $LiYF_4$ has also been frequently employed to fabricate lanthanide-doped upconversion crystals [8]. In contrast to $NaYF_4$ host matrix, $LiYF_4$ not only offers comparable emission intensity, but also generates additional emission lines [9]. Thus, $LiYF_4$ can provide us with a complementary host matrix to $NaYF_4$ for technical applications such as scintillation and tunable upconversion lasers [9b,10]. Despite the phenomenal growth in nanoparticle synthesis, there are relatively few reports on the synthesis of $LiYF_4$ nanoparticles due to formidable synthetic challenges. To the best of our knowledge, most $LiYF_4$ nanoparticles known to date have been synthesized by thermal decomposition [9]. Although this method enables the synthesis of monodisperse nanoparticles with high dispersability in organic solvents, the requirement of toxic rare-earth trifluoroacetate precursors and release of toxic byproducts raises issues of substantial environmental concern, thereby limiting its use for commercial purposes.

In this paper, we present a facile and relatively environmental-benign approach for the synthesis of monodisperse lanthanide-doped $LiYF_4$ nanoparticles. The synthetic strategy is based on the interaction of metal oleate with ammonium fluoride at room temperature and subsequent growth of the nanoparticles at elevated temperatures. We also show that multicolor tuning of the upconversion emission can be obtained by varying doping composition and concentration, while the size of the nanoparticles could be tuned by controlling the ratio of the fluoride to metal ions.

2. Experimental section

2.1. Materials

$YCl_3{\cdot}6H_2O$ (99.99%), $YbCl_3{\cdot}6H_2O$ (99.99%), $ErCl_3{\cdot}6H_2O$ (99.9%), $TmCl_3{\cdot}6H_2O$ (99.99%), $HoCl_3{\cdot}6H_2O$ (99.99%), LiOH (98%), NH_4F (98%), 1-octadecene (90%) and oleic acid (90%) were purchased from Sigma-Aldrich and used as starting materials without further purification.

2.2. Nanoparticle synthesis

In a typical experiment, 2 ml solutions of $RECl_3$ (0.2 M, RE = Y, Yb, Er, Ho and Tm) in methanol were added to a 50-ml flask containing 3 ml of oleic acid and 7 ml of 1-octadecene. The solution was heated to 150 °C for 30 min and then cooled to room temperature. Subsequently, 5 ml methanolic solution of NH_4F (1.6 mmol) and LiOH (1 mmol) was added to the flask and the resulting mixture was stirred for 30 min. After removal of the methanol by evaporation, the solution was heated to 290 °C in an argon atmosphere for 1.5 h and cooled to room temperature. The resulting nanoparticles with a narrow size distribution (about 21 nm) were precipitated by addition of ethanol, collected by centrifugation, washed with water and ethanol for several times, and redispersed in cyclohexane.

2.3. Characterizations

X-ray diffraction (XRD) analysis was carried out on a Siemens D5005 X-ray diffractometer with Cu Kα radiation (λ = 1.5406 Å). Transmission electron microscopic (TEM) measurements were carried out using a JEOL 2010 transmission electron microscope operating at an acceleration voltage of 200 kV. The luminescence spectra were obtained with a DM150i monochromator equipped with a R928 photon counting photomultiplier tube (PMT), in conjunction with a 980 nm diode laser. The decay curves of the $LiYF_4$ were measured with a customized UV to mid infrared phosphorescence lifetime spectrometer (FSP920-C, Edinburgh) equipped with a digital oscilloscope (TDS3052B, Tektronix) and a tunable mid-band OPO laser as an excitation source (410–2400 nm, Vibrant 355II, OPOTEK). All luminescence studies were carried out at room temperature.

3. Results and discussion

The size and morphology of the lanthanide-doped $LiYF_4$ nanoparticles were first studied by transmission electron microscopy (TEM). Fig. 1a shows a representative TEM micrograph of Yb/Er (18/2 mol %) co-doped nanoparticles with an average diameter of 21 nm. High-resolution TEM (HRTEM) image reveals the highly crystalline nature of the as-synthesized $LiYF_4$ nanoparticles (Fig. 1b). The HRTEM image also shows lattice fringes with observed *d*-spacings of 0.46 nm and 0.30 nm that respectively correspond to lattice spacings in the (011) and (103) planes of tetragonal-phase $LiYF_4$ (Fig. 1b). The electron diffraction pattern shown in Fig. 1c obtained from Fourier transform of the HRTEM image confirms the single-crystalline tetragonal-phase of the nanoparticle. Compositional analysis of an individual particle by energy-dispersive X-ray spectroscopy (EDX) reveals the presence of the doped elemental Yb and Er (Fig. 1d). The samples were further studied by XRD and shown in Fig. 1e. All diffraction peaks can be well indexed in accordance with tetragonal $LiYF_4$ crystal (JCPDS file No. 81-2254), indicating the formation of pure tetragonal-phase of the nanoparticles. Importantly, these nanoparticles are well dispersed in a variety of nonpolar solvents including hexane, cyclohexane, dichloromethane, and toluene.

The same synthetic procedure was further used to synthesize $LiYF_4$ nanoparticles doped with other lanthanide ions such as Yb/Tm (20/0.2 mol %) and Yb/Ho (18/2 mol %). TEM images in Fig. 2 a and b show that the size and morphology of the nanoparticles closely resemble to those of Yb/Er co-doped $LiYF_4$ nanoparticle counterpart. These results demonstrate that the variation of dopant ions in low concentrations does not alter the particle growth process. However, under identical experimental conditions, the size of the nanoparticles is found to be dependent on the ratio of fluoride (F^-) to rare-earth metal (RE^{3+}) ions. As shown in Fig. 2c and 2d, large nanoparticles of about 40 nm were obtained as the ratio of F^- to RE^{3+} reached 8/3. With increase in the F^- to RE^{3+} ratio, a decrease in particle size was observed. Ultra small nanoparticles of about 12 nm can be obtained when the F^- to RE^{3+} ratio reached 6.

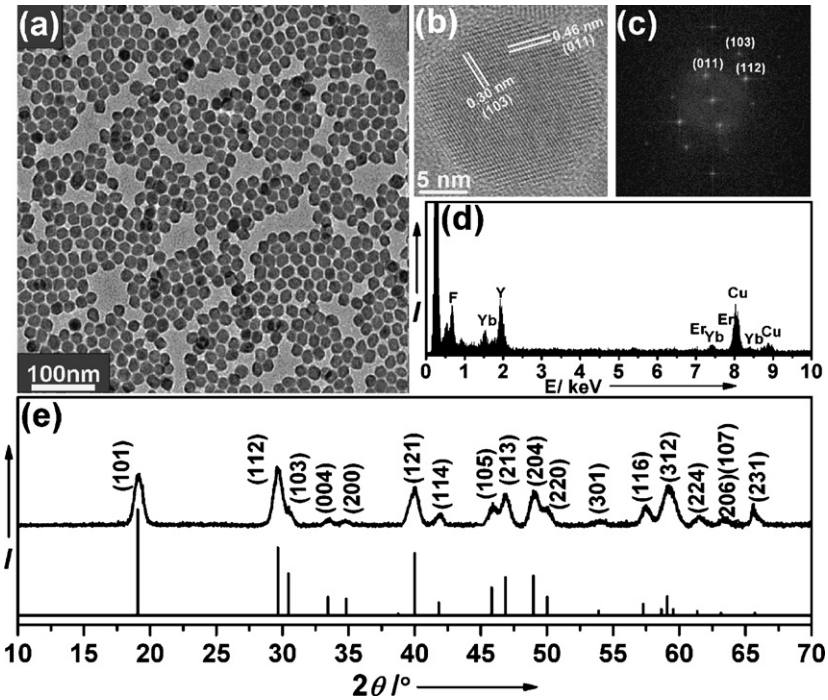

Fig. 1. (a) Low-resolution TEM image of the as-synthesized $LiYF_4$:Yb/Er (18/2 mol %) nanoparticles. (b) High-resolution TEM image of a nanoparticle taken in [311] incidence and (c) the corresponding Fourier-Transform diffractogram. (d) EDX analysis and (e) XRD pattern of the nanoparticles. Note that the Li ion is undetectable by EDX and the strong signals for Cu in (d) come from the copper TEM grid.

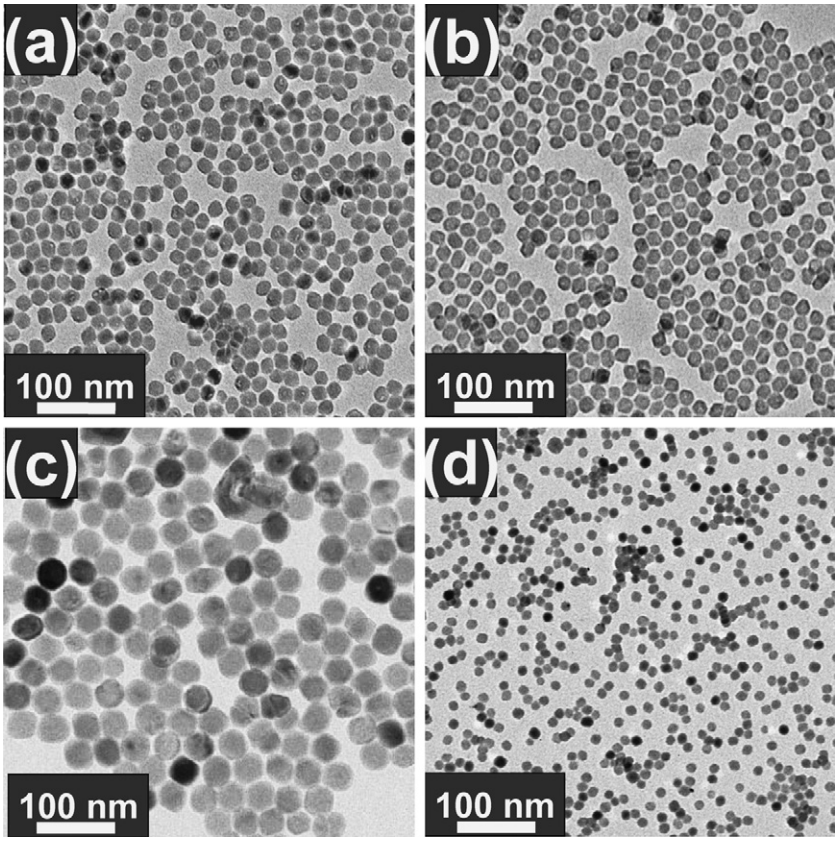

Fig. 2. TEM images of the as-synthesized nanoparticles with different doping compositions and metal-to-F ratios. (a) $LiYF_4$: Yb/Ho (18/2 mol %). (b) $LiYF_4$: Yb/Tm (20/0.2 mol %). (c) $LiYF_4$: Yb/Er (18/2 mol %) with a metal-to-F ratio of 3/8. (d) $LiYF_4$: Yb/Er with a metal-to-F ratio of 1/6.

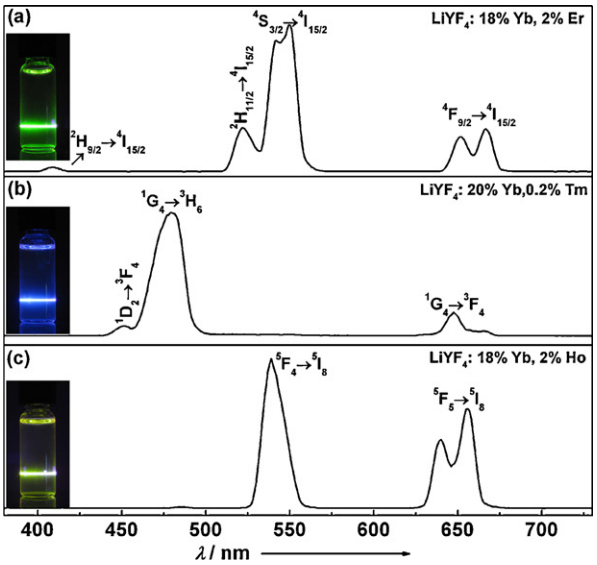

Fig. 3. Room-temperature upconversion emission spectra of $LiYF_4$ nanoparticles co-doped with (a) Yb/Er (18/2 mol %), (b) Yb/Tm (20/0.2 mol %), and (c) Yb/Ho (18/2 mol %). The samples were excited with a 980-nm diode laser operating at 600 mW. Inserts are digital camera photographs of corresponding solution samples.

The particle size variation as a function of F to rare-earth metal ratio can be explained by a crystallization speed-controlled model [11]. Because the particle growth was initiated with the reaction between the F^- ion and rare-earth oleate complex, a high concentration of F^- can significantly enhance particle crystallization rate. The crystallization acceleration effect related to high monomer concentration eventually leads to decreased critical size of the product [12].

Each lanthanide ion possesses a distinct set of energy levels that result in characteristic emissions at particular wavelengths. The upconversion emission from these nanoparticles can be readily manipulated by modifying doping compositions. Under excitation at 980 nm, the $LiYF_4$:Yb/Er (18/2 mol %) nanoparticles exhibit characteristic sharp emission peaks resulting from $^2H_{9/2} \rightarrow {}^4I_{15/2}$ (410 nm), $^2H_{11/2}, {}^4S_{3/2} \rightarrow {}^4I_{15/2}$ (525–540 nm), and $^4F_{9/2} \rightarrow {}^4I_{15/2}$ (660 nm) transitions of Er^{3+} (Fig. 3a). These emissions lead to an overall green color light (Fig. 3a, insert). In contrast, the $LiYF_4$:Yb/Tm (20/0.2 mol %) nanoparticles exhibit a blue color emission resulting from $^1D_2 \rightarrow {}^3F_4$ (450 nm), $^1G_4 \rightarrow {}^3H_6$ (475 nm), and $^1G_4 \rightarrow {}^3F_4$ (650 nm) transitions of Tm^{3+} while the $LiYF_4$: Yb/Ho (18/2 mol %) nanoparticles display a yellow color emission due to $^5F_4 \rightarrow {}^5I_8$ (525 nm), $^5F_5 \rightarrow {}^5I_8$ (650 nm) transitions of Ho^{3+} (Fig. 3 b and c).

It should be noted that the Yb^{3+} in the host lattice does not emit visible light. However, the Yb^{3+} makes a significant contribution to the upconversion emissions by acting as a sensitizer that strongly absorbs the excitation irradiation and then transfers the excitation energy to the emitters (Fig. 4a). The energy transfer process finds reflection as a rising edge in the luminescence decay curves (Fig. 4 b–d). The decay curves also showed a nearly single-exponential decay in the tail. By fitting with a single exponential function $I(t) = I_0 \exp(-t/\tau)$, the lifetimes for

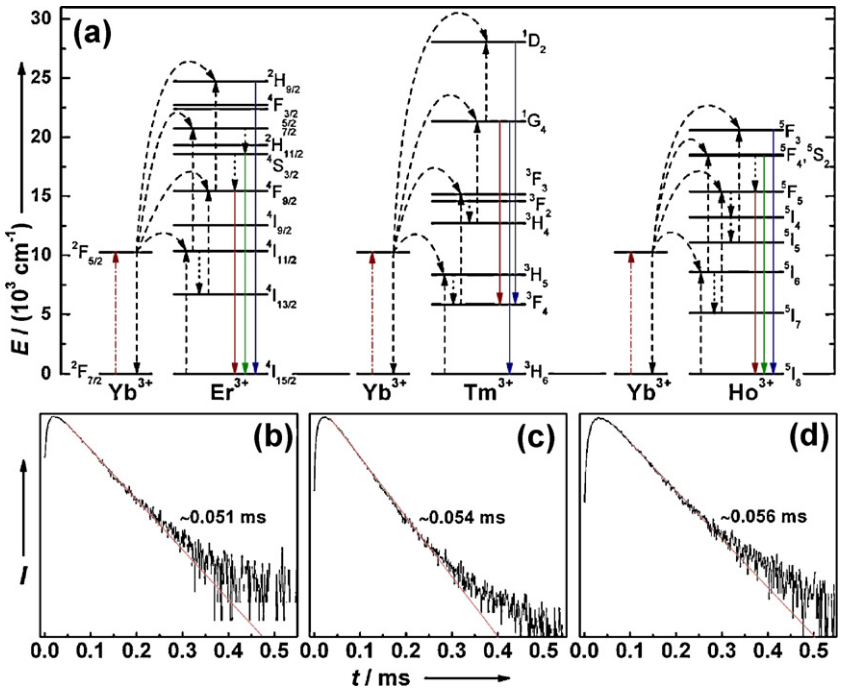

Fig. 4. (a) Schematic energy level diagrams showing typical UC processes for Yb^{3+}, Er^{3+}, Tm^{3+} and Ho^{3+}. The dashed-dotted, dotted, and full arrows represent excitation, multiphonon relaxation, and emission processes, respectively. (b–d) Luminescence decay curves of Er^{3+} in $LiYF_4$: Yb/Er (18/2 mol %) nanoparticles by monitoring the upconversion emission centered at 522 nm, 551 nm, and 669 nm. Flexible lines: experimental data; straight lines: fitting results by $I(t) = I_o \exp(-t/\tau)$ (I_o is the initial emission intensity at $t = 0$, and τ is the lifetime of the emission center).

$^2H_{11/2}$, $^4S_{3/2}$, $^4F_{9/2} \rightarrow {}^4I_{15/2}$ transitions of Er^{3+} are determined to be around 51, 54, and 56 μs, respectively. As expected, the luminescence lifetimes of $^2H_{11/2}$ and $^4S_{3/2}$ are the same since their populations are thermally coupled. The observed lifetimes for $^2H_{11/2}$, $^4S_{3/2} \rightarrow {}^4I_{15/2}$ transitions are basically consistent with those in the $NaYF_4$ counterparts, whereas much shorter lifetime for $^4F_{9/2} \rightarrow {}^4I_{15/2}$ transition is observed relative to that in $NaYF_4$ (~141 μs) [13]. The significant difference in lifetime for $^4F_{9/2} \rightarrow {}^4I_{15/2}$ transition may be ascribed to dissimilar crystal-field surroundings of Er^{3+} ions embedded in $LiYF_4$ and $NaYF_4$.

In a further set of experiments, we demonstrated that upconversion color tuning can be achieved by utilizing a three-component doping system in a dual emission process. Control of the doping concentration in the host lattice enables precise modulation of the relative intensities of upconversion emissions and thus the color output. For example, the $LiYF_4$ nanoparticles triply-doped with Yb/Er/Tm show dual emissions of Er^{3+} and Tm^{3+}. The relative intensity ratio of Er^{3+} and Tm^{3+} emissions can be manipulated by varying the doping concentration of Er^{3+} in the host lattice. In the absence of Er^{3+} dopant, the Yb/Tm co-doped nanoparticle system exhibits a blue color emission as previously discussed. Upon addition of a second emitter of Er^{3+} with increased dopant concentrations (0–1 mol %), the nanoparticle system exhibits significant changes in the green ($^2H_{11/2}$,$^4S_{3/2} \rightarrow {}^4I_{15/2}$) and red ($^4F_{9/2} \rightarrow {}^4I_{15/2}$) spectral region (Fig. 5a), resulting in tunable color output from blue to green (Fig. 5c–g).

Dual emission can also be achieved by simultaneously doping Tm and Ho in the host lattice. In comparison with Yb/Tm co-doped sample, the Yb/Tm/Ho triply-doped system exhibits additional emission peaks of Ho in the green and red spectral region (Fig. 5b). This dual emission process provides an alternative route towards upconversion multicolor tuning. As the doping concentration of Ho^{3+} increases, the colloidal solution of the triply-doped nanoparticles shows a notable color change (Fig. 5 h and i). The absence of quenching in the emission intensity as evidenced by the examination through the naked eye in all the triply-doped samples indicates that there is negligible energy transfer and cross relaxation between different types of activators. This phenomenon can be attributed to the low concentration (< 1 mol) of dopant emitter ions in the host lattice [14].

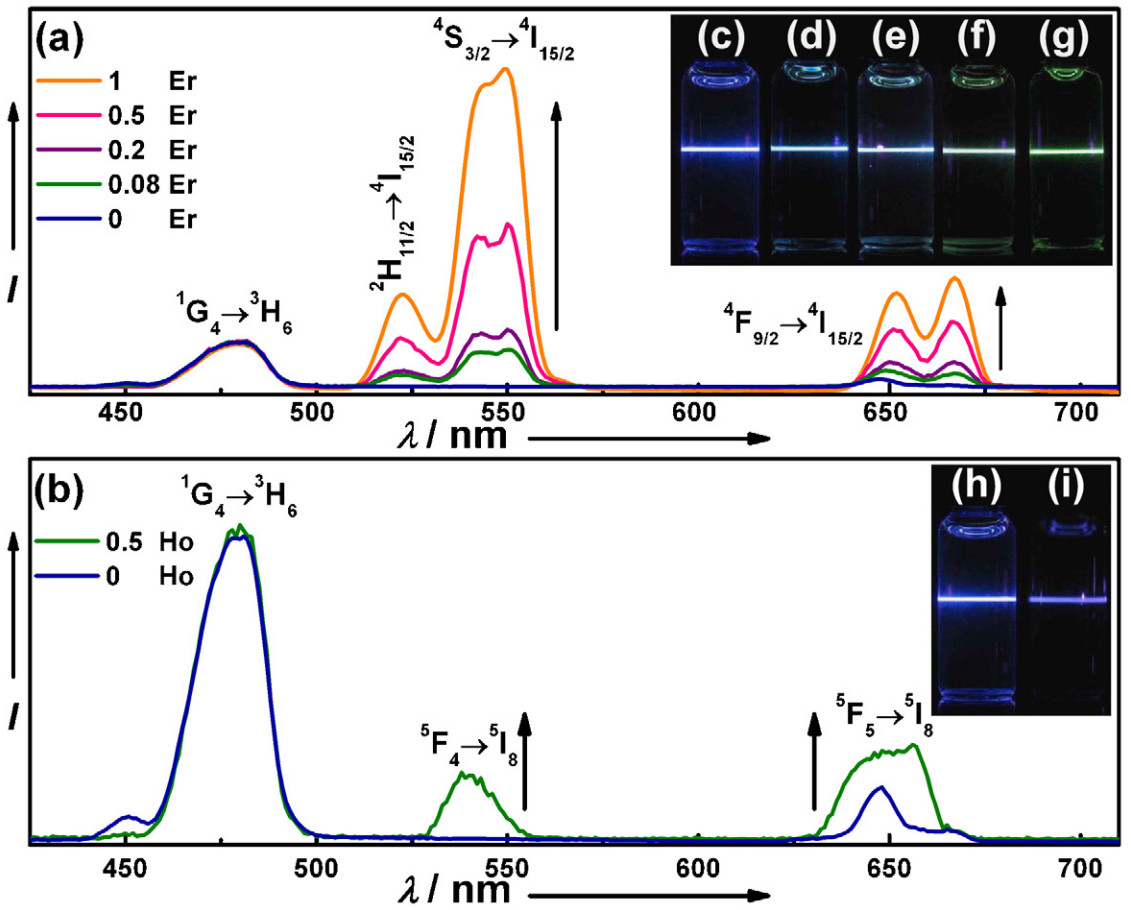

Fig. 5. Room temperature upconversion emission spectra of (a) $LiYF_4$: Yb/Tm/Er (20/0.2/0–1 mol %) and (b) $LiYF_4$: Yb/Tm/Ho (20/0.2/0–0.5 mol %) nanoparticles dispersed in cyclohexane solutions (8 mM). The spectra in (a) and (b) were normalized to Tm^{3+} 480 nm emission. (c–i) Compiled luminescent photos showing corresponding colloidal solutions of $LiYF_4$:Yb/Tm/Er (20/0.2/0–1 mol %) and $LiYF_4$:Yb/Tm/Ho (20/0.2/0–0.5 mol %), respectively.

4. Conclusions

In this work, tetragonal-phase $LiYF_4$ nanoparticles doped with upconverting lanthanide ions were synthesized by a novel solution-based method. Monodisperse nanoparticles with a tunable size can be readily obtained by varying the ratio of fluoride to rare-earth metal ions. The as-synthesized nanoparticles show intense upconversion emissions upon excitation at 980 nm.

The color output of the upconversion emission can be precisely manipulated by varying doping composition and concentration, providing potential applications for multiplex biological labeling and imaging.

Acknowledgements

X.L. acknowledges the Defence Science & Technology Agency (DSTA), the Singapore-MIT Alliance (SMA), and the Agency for Science, Technology and Research (A*STAR) for supporting this work. H.C. thanks the support from MOE (Grant No. ARC 27/07). X.C. acknowledges the support from the Hundreds of Talents Program of the Chinese Academy of Sciences (CAS), Instrument Developing Project of the CAS (Grant No. YZ200712), and the Key Project of International Cooperation of Fujian Province (Grant No. 2007I0024). We acknowledge Xiao Huang for high-resolution TEM Characterizations.

References

[1] (a) G. Blasse, B.C. Grabmaier, Luminescent Materials, Springer, Berlin, 1994;
(b) S.V. Eliseeva, J.-C.G. Bünzli, Chem. Soc. Rev. 39 (2010) 189;
(c) K. Binnemans, Chem. Rev. 109 (2009) 4283.
[2] (a) F. Wang, W. Tan, Y. Zhang, X. Fan, M. Wang, Nanotechnology 17 (2006) R1;
(b) F. Wang, X. Xue, X. Liu, Angew. Chem. Int. Ed. 47 (2008) 906;
(c) H.-T. Wong, H.L.W. Chan, J. Hao, Appl. Phys. Lett. 95 (2009) 022512;
(d) W. Luo, R. Li, X. Chen, J. Phys. Chem C 113 (2009) 8772.
[3] (a) F. Auzel, Chem. Rev. 104 (2004) 139;
(b) J.F. Suyver, A. Aebischer, D. Biner, P. Gerner, J. Grimm, S. Heer, K.W. Krämer, C. Reinhard, H.U. Güdel, Opt. Mater. 27 (2005) 1111;
(c) F. Wang, X. Liu, Chem. Soc. Rev. 38 (2009) 976.
[4] (a) E. Downing, L. Hesselink, J. Ralston, R. Macfarlane, Science 273 (1996) 1185;
(b) A. Shalav, B.S. Richards, M.A. Green, Sol. Energ. Mat. Sol. C 91 (2007) 829;
(c) F. van de Rijke, H. Zijlmans, S. Li, T. Vail, A.K. Raap, R.S. Niedbala, H.J. Tanke, Nat. Biotech. 19 (2001) 273;
(d) L. Wang, R. Yan, Z. Hao, L. Wang, J. Zeng, H. Bao, X. Wang, Q. Peng, Y. Li, Angew. Chem. Int. Ed. 44 (2005) 6054;
(e) Z. Chen, H. Chen, H. Hu, M. Yu, F. Li, Q. Zhang, Z. Zhou, T. Yi, C. Huang, J. Am. Chem. Soc. 130 (2008) 3023;
(f) H. Hu, L. Xiong, J. Zhou, F. Li, T. Cao, C. Huang, Chem. Eur. J. 15 (2009) 3577;
(g) F. Wang, Y. Han, C.S. Lim, Y.H. Lu, J. Wang, J. Xu, H.Y. Chen, C. Zhang, M.H. Hong, X.G. Liu, Nature 463 (2010) 1061.
[5] (a) A. Patra, C.S. Friend, R. Kapoor, P.N. Prasad, Appl. Phys. Lett. 83 (2003) 284;
(b) X. Mateos, M.C. Pujol, F. Güell, R. Solé, J. Gavaldà, J. Massons, M. Aguiló, F. Díaz, Opt. Mater. 27 (2004) 475;
(c) S.M. Kostritskii, D.B. Maring, R.F. Tavlykaev, R.V. Ramaswamy, Appl. Phys. Lett. 76 (2000) 2161;
(d) C. Jiang, F. Wang, N. Wu, X. Liu, Adv. Mater. 20 (2008) 4826.
[6] E. Pecoraro, D.F. de Sousa, R. Lebullenger, A.C. Hernandes, L.A.O. Nunes, J. Appl. Phys. 86 (1999) 3144.
[7] (a) S. Heer, K. Kömpe, H.U. Güdel, M. Haase, Adv. Mater. 16 (2004) 2102;
(b) G. Yi, H. Lu, S. Zhao, Y. Ge, W. Yang, D. Chen, L. Guo, Nano. Lett. 4 (2004) 2191;
(c) H. Mai, Y. Zhang, R. Si, Z. Yan, L. Sun, L. You, C. Yan, J. Am. Chem. Soc. 128 (2006) 6426;
(d) J.C. Boyer, F. Vetrone, L.A. Cuccia, J.A. Capobianco, J. Am. Chem. Soc. 128 (2006) 7444;
(e) L. Wang, Y. Li, Chem. Mater. 19 (2007) 727;
(f) F. Wang, X. Liu, J. Am. Chem. Soc. 130 (2008) 5642;
(g) L. Yang, H. Han, Y. Zhang, J. Zhong, J. Phys. Chem. C 113 (2009) 18995.
[8] (a) X.P. Chen, Q.Y. Zhang, C.H. Yang, D.D. Chen, C. Zhao, Spectrochim. Acta, Part A 74 (2009) 441;
(b) M. Pollnau, P.J. Hardman, W.A. Clarkson, D.C. Hanna, Optics Comm. 147 (1998) 203;
(c) S.A. Payne, L.K. Smith, W.L. Kway, J. Phys. Con. Matt. 4 (1992) 8525;
(d) A.W. Kueny, W.E. Case, M.E. Koch, J. Opt. Soc. Am. B 10 (1993) 1834;
(e) P.S. Golding, S.D. Jackson, T.A. King, Phys. Rew. B 62 (2000) 856;
(f) S. Kuck, I. Sokolska, Chem. Phys. Lett. 325 (2000) 263;
(g) S. Nicolas, E. Descroix, M.F. Joubert, Optic. Mater. 22 (2003) 139.
[9] (a) V. Mahalingam, F. Vetrone, R. Naccache, A. Speghini, J.A. Capobianco, Adv. Mater. 21 (2009) 4025;
(b) V. Mahalingam, R. Naccache, F. Vetrone, J.A. Capobianco, Chem. Eur. J. 15 (2009) 9660;
(c) G.S. Yi, W.B. Lee, G.M. Chow, J. Nanosci. Nanotech. 7 (2007) 2790;
(d) Y. Du, Y. Zhang, L. Sun, C. Yan, Dalton. Trans. (2009) 8574.
[10] S. Nicolas, E. Descroix, M.F. Joubert, Y. Guyot, M. Laroche, R. Moncorge, R.Y. Abdulsabirov, A.K. Naumov, V.V. Semashko, A.M. Tkachuk, M. Malinowski, Opt. Mater. 22 (2003) 139.
[11] C. Liu, H. Wang, X. Li, D. Chen, J. Mater. Chem. 19 (2009) 3546.
[12] Y. Yin, A.P. Alivisatos, Nature 437 (2005) 664.
[13] C.X. Li, Z.W. Quan, J. Yang, P.P. Yang, J. Lin, Inorg. Chem. 46 (2007) 6329.
[14] F. Wang, J. Wang, J. Xu, X. Xue, H. Chen, X. Liu, Spectrosc. Lett. (In press).